Redox-Induced Conformational Changes in Myoglobin and Hemoglobin: Electrochemistry and Ultraviolet–Visible and Fourier Transform Infrared Difference Spectroscopy at Surface-Modified Gold Electrodes in an Ultra-Thin-Layer Spectroelectrochemical Cell†

Daniela D. Schlereth* and Werner Mäntele

Institut für Biophysik und Strahlenbiologie der Universität Freiburg, Albertstrasse 23, 7800 Freiburg, Germany

Received March 5, 1992; Revised Manuscript Received May 28, 1992

ABSTRACT: Using suitable surface-modified electrodes, we have developed an electrochemical system which allows a reversible heterogeneous electron transfer at high (≈5 mM) protein concentrations between the electrode and myoglobin or hemoglobin in an optically transparent thin-layer electrochemical (OTTLE) cell. With this cell, which is transparent from 190 to 10 000 nm, we have been able to obtain electrochemically-induced Fourier-transform infrared (FTIR) difference spectra of both proteins. Clean protein difference spectra between the redox states were obtained because of the absence of redox mediators in the protein solution. The reduced-minus-oxidized difference spectra are characteristic for each protein and arise from redox-sensitive heme modes as well as from polypeptide backbone and amino acid side chain conformational changes concomitant with the redox transition. The amplitudes of the difference bands, however, are small as compared to the total amide I absorbance, and correspond to approximately 1% (4%) of the reduced-minus-oxidized difference absorbance in the Soret region of myoglobin (hemoglobin) and to less than 0.1% of the total amide I absorbance. Some of the bands in the 1560–1490-cm^{-1} spectral regions could be assigned to side-chain vibrational modes of aromatic amino acids. In the conformationally sensitive spectral region between 1680 and 1630 cm^{-1}, bands could be attributed to peptide C=O modes because of their small (2–5 cm^{-1}) shift in ^2H_2O. A similar assignment could be achieved for amide II modes because of their strong shift in ^2H_2O. On the basis of their vibrational frequency and structural arguments, a part of these signals is attributed to α-helical regions of the proteins. Although the band assignment is far from being complete, the results demonstrate that FTIR spectroelectrochemistry can be used as a technique for dynamic and structural studies of redox proteins under near-native conditions in aqueous solution.

Myoglobin as well as hemoglobin is very well known to undergo irreversible heterogeneous electron transfer reactions at bare metallic electrodes such as mercury (Scheller et al., 1975), gold (Stargardt et al., 1978), platinum (Song & Dong, 1988), or silver (Cotton et al., 1980). However, much effort has been devoted to obtain *biocompatible* electrodes based on the metal surface modification with a dye, in order to get reversible heterogeneous electron transfer processes with both proteins (Stargardt et al., 1978; Ye & Baldwin, 1988; Song & Dong, 1988; Dong et al., 1989; Zhu & Dong, 1990).

In contrast to cytochrome *c*, which develops reversible heterogeneous electron transfer at a wide variety of modified electrode surfaces (di Gleria et al., 1986; Hill & Lawrance, 1989; Barker et al., 1990), myoglobin and hemoglobin undergo a quasi-reversible electrochemical response with reaction rates of the oxidation much slower than the reduction. The only exception is the electrochemistry of hemoglobin at Janus green modified platinum electrodes, which exceptionally show the opposite behavior (Zhu & Dong, 1990).

While in cytochrome *c* the homogeneous electron transfer reaction proceeds via a plane equatorial to the heme ring, electron transfer in myoglobin involves the sixth coordination position of the heme iron and thus proceeds via a plane perpendicular to the heme ring (Castner & Hawkridge, 1983). This site in myoglobin is much more buried with respect to the protein surface than in cytochrome *c*, and thus its interaction with the electrode surface is hindered (Stellwagen, 1978). For hemoglobin the situation is even worse, since it is a tetramer with four heme moieties which must interact with the electrode.

On the other hand, these surface-modified electrodes have been successfully used in order to reduce and reoxidize very dilute samples with protein concentrations of about 50 μM, and even in such cases either a progressive poisoning of the electrode arising from to protein adsorption (Castner & Hawkridge, 1983) or a modifier leaking during usage (Song & Dong, 1988; Dong et al., 1989) led to short-lived electrodes.

Poisoning of the electrode represents a crucial problem for experiments in which the protein concentration reaches 5–10 mM. Concentrations in this range, however, are necessary to record infrared spectra [using Fourier transform infrared (FTIR)[1] spectroscopy] using an ultra-thin-layer electrochemical cell as recently developed by us (Moss et al., 1990). Moreover, reduction and reoxidation of these highly concentrated samples should be possible in a quantitative and reversible electrochemistry. The extreme sensitivity of FTIR difference spectroscopy leads to the detection of individual bonds even in these macromolecules; however, it requires that this reduction or oxidation should be performed in a moderately

† D.S. gratefully acknowledges a postdoctoral fellowship from the Spanish Consejo Superior de Investigaciones Cientificas. W.M. is indebted to the Deutsche Forschungsgemeinschaft for financial support (Ma 1054/2-2 and 5-1) and a Heisenberg Fellowship.

[1] Abbreviations: FTIR, Fourier transform infrared; OTTLE, optically transparent thin-layer electrochemical cell; SME, surface-modified electrode; BCB, brilliant cresyl blue; MB, methylene blue; JG, Janus green; MV, methyl viologen; $E_{50\%}$, 50% reduction potential; $E_{1/2}$, midpoint potential; E_{pc}, cathodic peak potential; E_{pa}, anodic peak potential.

0006-2960/92/0431-7494$03.00/0

short time (5–15 min) for reasons of stability. An additional requirement is to avoid large reduction overpotentials exceeding –600 mV (vs Ag/AgCl), at which a slight hydrogen evolution may occur.

The motivation for the study of the conformational changes concomitant with the oxidoreduction of the prosthetic groups in myoglobin and hemoglobin relies on the fact that a very close similarity has been found between the oxygenation and the redox equilibria (Antonini et al., 1964; Brunori et al., 1964). Thus, a similar conformational change may be expected after the reactions of oxygen binding or the oxidation of the heme iron. In fact, it has been shown that the conformations of methemoglobin and oxygenated hemoglobin are similar (Banerjee & Cassoly, 1969b).

The oxidation reaction results in a transition from the nonligated five-coordinated myoglobin or hemoglobin to the ligated six-coordinated protein. The difference with respect to the physiological reaction, besides the oxidation state of the heme iron, is that in metmyoglobin as well as in methemoglobin the sixth coordination site is occupied by a water molecule instead of an oxygen molecule.

The oxygen binding is accompanied by shortening of the Fe–N bonds, a shift of the iron out of the heme plane, and the movement of the helix F toward the heme plane. The heme propionates which link the heme to the protein by salt bridges seem to act as stabilizers of a specific heme conformation and can be broken easily to allow the rotation of the heme around the Fe–N_ϵ(His-64) bond (La Mar et al., 1991).

Even though there are some differences in heme orientation and in several details of the tertiary structure between myoglobin and the α and β chains of hemoglobin arising from the differences in their amino acid sequences (Dayhoff, 1972), myoglobin has been extensively used as a model for the tertiary structure conformational change produced upon oxygen binding in each subunit of hemoglobin.

Crystallographic data have shown that the changes produced upon oxygenation in myoglobin were larger (Phillips, 1980) than those found between myoglobin and metmyoglobin (Takano, 1977a,b). However, the possibility was suggested that these differences could arise from differences in the pH used by the two authors (8.4 and 5.7, respectively). Thus, we can consider that the tertiary structures of oxymyoglobin and metmyoglobin are extremely close.

The stereochemistry of the heme–O_2 complex in myoglobin and hemoglobin has been extensively studied by resonance Raman spectroscopy. These studies are based on the observed shifts of the Fe-N_ϵ (His-F8) stretching mode (Spiro et al., 1990) and the study of the heme modes after oxygen flash photolysis (Stein et al., 1982).

The geometry of the heme complex of hemoglobin closely resembles that of myoglobin. Even though most of the heme contact groups are identical, there are some differences arising from the different amino acid sequence of myoglobin and the α and β chains of hemoglobin. These changes may be responsible for the different oxygen affinity of each complex (Antonini et al., 1965). It is remarkable that some features of the oxidation equilibrium in hemoglobin have been explained on the basis of the hetereogeneity of the α and β chains (Brunori et al., 1967) and that the isolated subunits show different values of their standard redox potentials (Banerjee & Cassoly, 1969a).

There are, however, some differences in the active sites of the α and β chains which cannot be explained on the basis of the small differences between their heme complexes and may arise from a cumulative effect of all the differences in the amino acid sequence. The main consequence is that the β subunits seem to have more space to accommodate the oxygen molecule as compared to α-hemoglobin and myoglobin, which results in a lower oxygen affinity (Shaanan, 1983).

The three-dimensional structures derived from X-ray crystallography reflect a static picture of the (crystalline) state of the protein but lack dynamic or functional information. They need to be complemented by spectroscopic techniques which allow study of the proteins in solution and may be a better approach for understanding the dynamics of biochemical processes, where the proteins maintain their native conformations.

In the work presented here, we have investigated the electrochemical properties of different surface-modified gold minigrid electrodes in order to get quasi-reversible heterogeneous electron transfer reactions with myoglobin and hemoglobin at high protein concentrations. We have used these electrodes in an ultra-thin-layer electrochemical cell for the study of the conformational changes produced upon oxidoreduction of the heme group by FTIR difference spectroscopy.

MATERIALS AND METHODS

(*1*) *Sample Preparation.* The ultra-thin-layer electrochemical cell suitable for UV/vis and IR spectroscopy of proteins in aqueous solvents has been described previously (Moss et al., 1990) and used with minor modifications as described by Baymann et al. (1991). As an essential feature of this cell, the protein solution forms a 10–15-μm layer on a 70% transparent gold grid working electrode (Buckbee-Mears, St. Paul, MN) between two calcium fluoride windows, in electrical contact with a platinum foil counterelectrode and an Ag/AgCl/3 M KCl reference electrode.

Horse skeletal muscle myoglobin or human blood hemoglobin (both obtained from Sigma) were prepared at concentrations between 50 and 150 mg/mL in 100 mM phosphate buffer, pH 7, containing 100 mM KCl as supporting electrolyte. The gold grid working electrode was freshly modified before each experiment following the procedures described below and rinsed thoroughly afterward with distilled water to avoid the presence of modifier in the protein solution. Filling of the cell was performed according to the procedure described by Moss et al. (1990).

(*2*) *UV–vis Spectroscopy and Electrochemistry.* The equipment used for chronoamperometry, cyclic voltammetry, and coulometry was constructed in our laboratory according to standard designs. UV-vis spectra were recorded on a remodeled Cary 14 specrophotometer or on a single-beam spectrophotometer built to our design. Both spectroscopy in the 350–700–nm region and electrochemistry were controlled through interfaces from data acquisition and treatment software (MSPEK) developed in our laboratory by D. Moss and S. Grzybek. All potentials quoted in this work are given vs Ag/AgCl/3 M KCl (add 208 mV for potentials vs standard hydrogen electrode).

The time required to obtain the full oxidation and reduction of the samples at a constant applied potential was determined following the time-dependent absorbance change at 438 nm for myoglobin and at 434 nm for hemoglobin. Potential stepping curves were drawn from the absorbance values at the same wavelengths obtained after the equilibration of the cell at a given potential (the equilibrium time was determined as the time required to reach a constant and background-limited current value). For reductive potential stepping curves, increasingly more negative potentials were applied during 100 s after full oxidation of the sample at +500 mV after each step. For oxidative stepping curves, increasingly more positive

potentials were applied for 200 s after full reduction of the sample at –400 mV after each step. All electrochemical measurements were performed at room temperature.

(*3*) *Gold Grid Electrode Modification.* All procedures for gold modification described in this work are based on the adsorption of dyes onto the gold grid surface in order to obtain a surface-modified electrode (SME) which allows us to obtain quantitative and quasi-reversible electrochemistry with short equilibration times for an applied potential. The latter requirement is essential for FTIR difference spectroscopy, since the spectra of the two different redox states need to be recorded in rapid succession, i.e., within ca. 10–15 min to enable calculation of difference spectra at a sensitivity of ca. 10^{-4} absorbance units, corresponding to the contributions from individual bonds.

(*a*) *Methyl viologen modified electrodes* (*MV-SMEs*) were prepared by introducing the electrode into a 1 mM solution of MV in 100 mM phosphate buffer and 100 mM KCl, pH 7.0, and applying during 5 min a potential of –950 mV, followed by a potential step at +200 mV for 10 min as described by Landrum et al. (1977). These electrodes were tested with myoglobin as described by Bowden et al. (1980).

(*b*) *Methylene blue modified electrodes* (*MB-SMEs*) were prepared by cyclic scanning of a 1 mM MB solution in 100 mM phosphate buffer and 100 mM KCl, pH 7.0, between +500 and –600 mV in the electrochemical cell for 60 min. The modification was monitored by following the decrease of the current in the cyclic voltammogram of the dye, assuming the modification process to be complete when the voltammograms showed a backgroundlike voltammetric response. After thorough rinsing with distilled water, these electrodes were tested with 100 mg/mL solutions of both proteins.

(*c*) *Janus green modified electrodes* (*JG-SMEs*) were prepared by dip coating of the electrode in a 1 mM solution of Janus green in 100 mM phosphate buffer and 100 mM KCl, pH 7.0, during 5 min, as described by Zhu and Dong (1990). These electrodes were tested with a 100 mg/mL hemoglobin solution.

(*d*) *Brilliant cresyl blue modified electrodes* (*BCB-SMEs*) were prepared by cyclic scanning of a 1 mM solution of BCB, analogous to preparation of MB-SMEs. After thorough rinsing with distilled water, these electrodes were tested with 100 mg/mL solutions of both proteins.

(*4*) *FTIR Difference Spectroscopy.* The reaction mixture for the FTIR experiments consisted of highly concentrated protein solutions (150 and 50 mg/mL for myoglobin and hemoglobin, respectively) in 100 mM potassium phosphate buffer, pH 7, containing 100 mM KCl. Samples in heavy water were prepared with the same salt concentrations at a pD of 7.4. All spectra shown in this paper were recorded at 5 °C and were the average of 32 scans at 3 scans/s on a Bruker IFS 25 FTIR spectrophotometer equipped with a MCT detector of selected sensitivity. The FTIR spectrophotometer was modified in order to allow the measuring beam of the single-beam spectrophotometer for visible light to pass coaxially through the sample, thus allowing simultaneous recording of the UV–vis and IR spectra. IR difference spectra were calculated from single-beam-spectra (I_1, I_2) of the sample equilibrated at the different potentials by forming $A = \log (I_2/I_1)$. No baseline subtractions or weighted subtractions of buffers were performed.

Table I: Electrochemical Response of Myoglobin and Hemoglobin at the Different SMEs

electrode	protein, concn	reduction potential, time	oxidation potential, time
MV-SME	myoglobin, 30 mg/mL	–650 mV, 300 s	+500 mV, 300 s
BCB-SME	myoglobin, 100 mg/mL	–400 mV, 100 s	+500 mV, 200 s
JG-SME	hemoglobin, 100 mg/mL	–400 mV, 300 s	+500 mV, 50 s
MB-SME	myoglobin, 100 mg/mL	–400 mV, 100 s	+500 mV, 200 s
MB-SME	hemoglobin, 100 mg/mL	–300 mV, 100 s	+500 mV, 300 s

RESULTS

(*I*) *Electrochemistry and UV–vis Spectroscopy*

The electrodes response with different modifications and the overpotentials required for each protein are summarized in Table I.

Methyl Viologen Modified Electrodes (*MV-SMEs*). A 30 mg/mL myoglobin sample was completely reduced after 300 s at –650 mV and reoxidized after 300 s at +500 mV. At higher concentrations, MV-SMEs became quickly poisoned, resulting in a complete and irreversible reduction of the protein. These conditions are not suitable for an FTIR experiment because they allow only poorly concentrated samples and require a high reduction overpotential. Due to the fact that the interaction of hemoglobin with the electrode is much poorer, no attempts were done with hemoglobin.

Brilliant Cresyl Blue Modified Electrodes (*BCB-SMEs*). A 100 mg/mL myoglobin sample was fully reduced after 100 s at –400 mV and reoxidized after 200 s at +500 mV. At pH 7.0, when stepping during 100 s at increasingly more negative potentials, myoglobin starts to become reduced at –100 mV. Fifty percent reduction was obtained at $E_{50\%} = -270$ mV.

The midpoint potential of BCB on the gold electrode was determined by cyclic voltammetry, giving a value of $E_{1/2} = -260$ mV ($E_{pc} - E_{pa} = 60$ mV, scan rate 1 mV/s) at pH 7.0. The standard redox potential of myoglobin at the same pH is 98 mV more positive (Ye & Baldwin, 1988). Thus, it seems that the reduction of the protein only takes place after the reduction of the layer of adsorbed modifier, suggesting the same electron transfer mechanism as proposed by Dong et al. (1989) for the electrochemical reaction of hemoglobin at BCB-modified platinum electrodes.

With highly concentrated samples of hemoglobin, the electrode did not show a stable response. Poisoning of the electrode by strong protein adsorption coupled with leaking of the modifier from the electrode surface could be the reason for this behavior.

Janus Green Modified Electrodes (*JG-SMEs*). With JG-SMEs, a 100 mg/mL hemoglobin sample could be fully reduced after 300 s at –400 mV and subsequently reoxidized after 50 s at +500 mV. When successive 100-s reductive steps at increasingly more negative potentials were applied, a Nernstian curve was obtained with an $E_{50\%}$ value at –290 mV. The oxidative process followed by the application of increasingly more positive potentials during 50 s showed a large hysteresis. About 15% of the total protein was oxidized when the potential had reached 0 mV, and bulk oxidation occurred between 0 and +300 mV.

The slower reduction process at the gold minigrid JG-SMEs agrees with the behavior of hemoglobin at platinum JG-SMEs described by Zhu and Dong (1990), leading to the requirement of highly negative overpotentials in order to obtain fast reduction rates. On the other hand, gold JG-SMEs proved to be very unstable, giving rise to slower reaction rates, both in the reduction and in the oxidation process, just after the first reductive–oxidative cycle. Because of this disadvantage

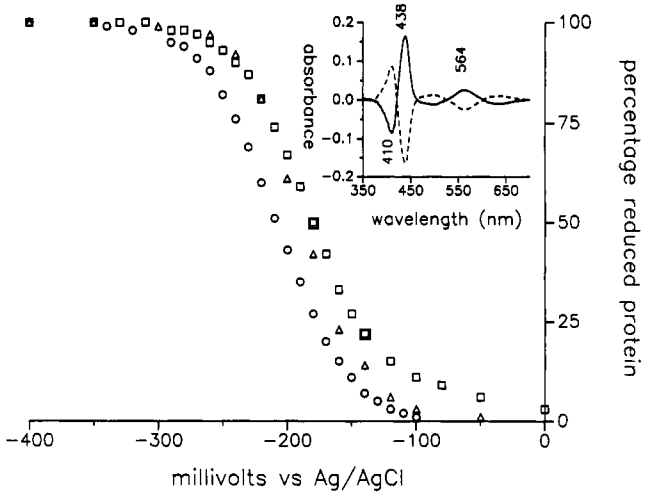

FIGURE 1: Percentage of reduced protein vs applied potential. Conditions: 100 mg/mL myoglobin in phosphate buffer and 100 mM KCl, pH 7.0 O, 100-s reductive steps; Δ, 200-s reductive steps; □, 200-s oxidative steps. Inset: UV–vis difference spectra of the same sample, (—) reduced-minus-oxidized and (- - -) oxidized-minus-reduced. The reduction of the sample was achieved after 200 s at –400 mV and the reoxidation after 300 s at +500 mV.

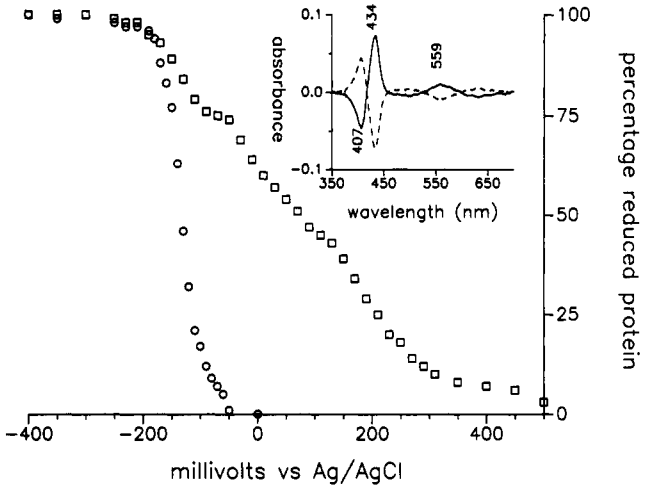

FIGURE 2: Percentage of reduced protein vs applied potential. Conditions: 50 mg/mL hemoglobin in phosphate buffer and 100 mM KCl, pH 7.0. O, 100-s reductive steps; □, 200-s oxidative steps. Inset: UV–vis difference spectra of the same sample, (—) reduced-minus-oxidized and (- - -) oxidized-minus-reduced. The reduction of the sample was achieved after 200 s at –300 mV and the reoxidation after 300 s at +500 mV.

and the high reduction overpotentials required, no attempts were made with myoglobin.

Methylene Blue Modified Electrodes (MB-SMEs). MB-SMEs turned out to be the most appropriate type of electrode for a quantitative, reversible, and rapid electrode reaction of both proteins. Complete reduction of a 100 mg/mL myoglobin sample was obtained after 100 s at –400 mV. Reoxidation was complete after 200 s at +500 mV. For a 100 mg/mL hemoglobin sample, complete reduction was obtained after 100 s at –300 mV and full reoxidation after 300 s at +500 mV.

Figure 1 shows the potential stepping curve obtained for myoglobin after stepping for 100 s the potential at increasingly more negative values, and the reverse process obtained with 200-s steps at increasingly more positive potentials. Nernst functions are obtained for myoglobin in the reductive as well as in the oxidative process. Under these conditions, myoglobin is beginning to reduce at –100 mV and the $E_{50\%}$ value is obtained at –210 mV, slightly more positive as compared to the midpoint potential of methylene blue on gold electrodes determined by cyclic voltammetry ($E_{1/2}$ = –225 mV, $E_{pc} - E_{pa}$ = 70 mV, scan rate 1 mV/s) but with a reduction overpotential at 48 mV with respect to the standard redox potential of myoglobin at the same pH ($E°$ = –162 mV; Ye & Baldwin, 1988). When the reduction time in the reductive stepping curve was increased to 200 s, $E_{50\%}$ was shifted to –190 mV. The oxidative stepping curve, however, gave an $E_{50\%}$ value of –180 mV, indicating a slightly slower oxidation rate.

Figure 2 shows the reductive potential stepping curve obtained for hemoglobin after stepping for 100 s the potential at increasingly more negative values, and the reverse process after 200-s steps at increasingly more positive potential values. Hemoglobin is beginning to reduce at –50 mV, showing the $E_{50\%}$ at –140 mV, corresponding to 102 mV overpotential of reduction with respect to the standard redox potential of hemoglobin at this pH, $E°$ = –38 mV (Ye & Baldwin, 1988). The curve obtained for the reductive process is also a Nernst curve but steeper than the one obtained with myoglobin. The oxidative process shows a rather complicated pattern, with the oxidation being extremely delayed. The curve form indicates the overlapping of at least three redox processes. The first oxidation step, which is also the best defined, also exhibits an $E_{50\%}$ value at 140 mV. While the reductive stepping curves were very reproducible, the oxidative stepping curves were considerably influenced by the electrode surface conditions, mostly by the time-dependent electrode degradation.

(II) FTIR Difference Spectroscopy

We have shown that both myoglobin and hemoglobin at high concentrations react quantitatively and reversibly at MB-SMEs in the thin-layer electrochemical cell designed for UV–vis and IR spectroscopy. We now use this "electrochemical triggering" for the redox transition to generate the vibrational IR oxidized-minus-reduced difference spectra in order to detect the changes of molecular geometry and interaction with the redox transition of the heme(s).

We would like to emphasize that the redox reactions in the OTTLE cell have been achieved without the use of mediators added to the protein solutions. Thus, no contributions other than from the protein are expected. Since, however, there is a slight chance that a fraction of the adsorbed surface modifier might leak from the electrode surface and thus would be present in the protein solution (although in homeopathic concentrations), a blank spectrum is shown in Figure 4a. With the exception of the region around 1650 cm^{-1}, where minute noise is present due to the strong water adsorption, this baseline is perfectly flat. Thus, even minor bands in the IR difference spectra which are not discussed here arise from the protein conformational change.

The IR difference spectra of myoglobin and of hemoglobin in ^1H_2O and in ^2H_2O will be discussed separately. The major peaks are summarized in Tables II and III together with the proposed band assignments.

Infrared Spectroscopy of Myoglobin. For the recording of myoglobin IR difference spectra, the BCB-SMEs were used. A 150 mg/mL sample was first equilibrated at +500 mV for 5 min. After this, an IR single-beam spectrum of the oxidized state was recorded as a reference. A reducing potential of –300 mV was then applied for 200 s, and the IR spectrum of the reduced state was recorded. Figure 3a (solid line) shows the reduced-minus-oxidized FTIR difference spectrum of myoglobin in ^1H_2O. The reverse spectrum was obtained by equilibration of the sample at –300 mV, recording of the IR spectrum of the reduced state, application of an oxidizing

Table II: Myoglobin

wavenumber (cm^{-1})		
^1H_2O	^2H_2O	assignment
1684 (+) w	1680 (+) w	symmetric stretching of protonated
1700 (–) w	1696 (–) w	–COOH of heme-6 propionic acid
1664 (–) s	1662 (–) s	
1640 (+) s	1640 (+) s	(amide I)
1654 (–) m	1654 (–) s	
1630 (+) m	1630 (+) s	
1606 (+) w	1596 (–) w	
1582 (–) w	1570 (–) w	
1564 (–) w		
1548 (+) w	1548 (+) m	
1530 (+) m	1434 (+) w	(amide II)
	1448 (–) w	
1514 (+) w		phenol ring vibration of tyrosine
1500 (+) w		aromatic ring vibration of phenylalanine
	1196 (–) w	
1172 (–) w	1172 (–) w	histidine/Fe(III)–porphyrin complex
1148 (–) w	1150 (–) w	
1106 (+) m		
1100 (–) m	1100 (–) s	Fe(III)–porphyrin/histidine complex
1088 (+) m		

Table III: Hemoglobin

wavenumber (cm^{-1})		
^1H_2O	^2H_2O	assignment
1690 (+) w	1692 (+) w	antisymmetric stretching of protonated –COOH of heme-6 propionic acid
1668 (–) s	1674 (–) s	(amide I)
	1658 (–) vs	
1658 (+) m		
1631 (+) vs	1628 (+) vs	
1610 (–) s	1608 (–) vs	–CH=HC– stretching of aromatic or heme vinyls
1596 (–) m		
1578 (–) m	1574 (–) s	
1556 (+) s	1554 (+) s	indole ring vibration of tryptophan
1538 (+) m	1462 (+) m	(amide II)
	1440 (+) m	
1508 (+) m		phenol vibration of tyrosine or ring vibration of phenylalanine
1444 (–) m		
1434 (+) w		
1410 (+) m		
	1412 (+) m	
	1392 (–) m	
	1352 (–) m	
1316 (+) m	1316 (+) m	
	1264 (+) m	
	1248 (–) m	
1234 (–) m	1234 (–) m	
1170 (–) w	1170 (–) w	
1146 (–) w	1148 (–) w	Fe(III)–porphyrin–histidine complex
1106 (–) m		

potential of +500 mV for 300 s, and recording of the IR spectrum of the oxidized state. This oxidized-minus-reduced difference spectrum (Figure 3a, dotted line) is the exact mirror image of the first spectrum, thus demonstrating full reversibility of the redox-induced molecular changes.

Only a small section of the IR difference spectrum is displayed in Figure 3; however, the full range of 4000–1000 cm^{-1} was recorded. Although sharp differential features (reversible and highly reproducible) were detected in the 3000–2500-cm^{-1} range, we focus here on the 1800–1000-cm^{-1} range, containing most if not all of the diagnostically relevant bands. Both the forward (Figure 3a, solid line) and the reverse (Figure 3a, dotted line) difference spectra were obtained for many different samples. The application of intermediate potentials yielded the same band pattern at intermediate amplitudes. All bands titrate in unison; the titration of the infrared signals closely corresponds to the titration of the heme band at 438 nm with an $E_{50\%} = -270$ mV. The same spectra were obtained with the MB-SME (data not shown). For all spectra shown, the amplitude of the main infrared difference signal [1644 cm^{-1} (–)/1640 cm^{-1} (+)] was at most 1% of the reduced-minus-oxidized absorbance difference of the Soret band at 438 nm.

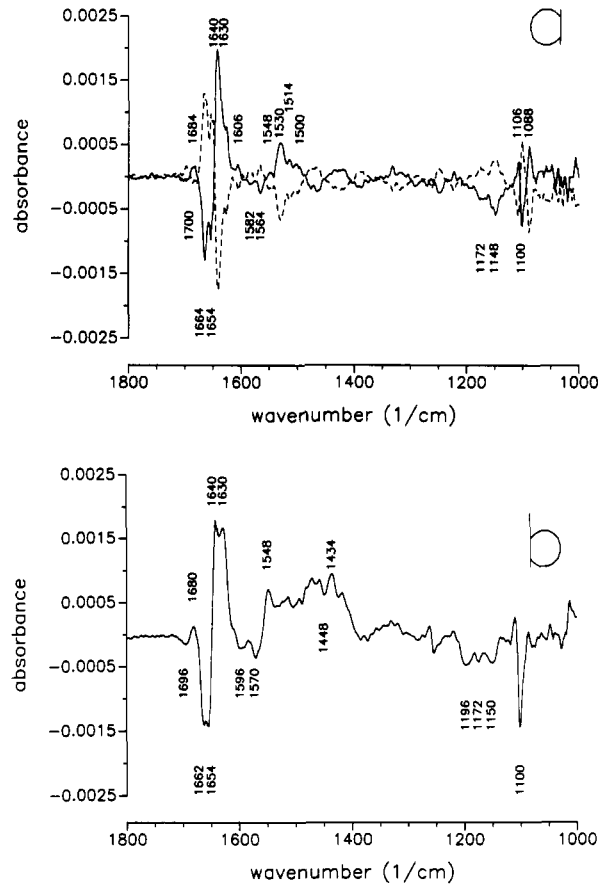

FIGURE 3: (a) (—) Reduced-minus-oxidized and (- - -) oxidized-minus-reduced IR difference spectra of a 150 mg/mL myoglobin sample in phosphate buffer and 100 mM KCl, pH 7.0. The spectrum is the average of several electrolysis cycles of 200 s at –400 mV and 300 s at +500 mV. (b) Reduced-minus-oxidized IR difference spectra in ^2H_2O (same conditions as in panel a).

Suspension of the myoglobin in ^2H_2O, followed by equilibration at room temperature for 1 h, should lead to replacement of all exchangeable (i.e., N-, S-, and O-bound) protons by ^2H. Indeed, the FTIR difference spectrum in ^2H_2O (Figure 3b) shows distinct changes of band amplitudes and positions as compared to the spectrum in Figure 3a (solid line). In addition, the lower background absorbance between 1620 and 1670 cm^{-1} for the ^2H_2O sample leads to a lower noise level.

Infrared difference spectra of myoglobin show only a few bands of high intensity (Figure 3a). The main difference band structure in ^1H_2O at 1664 cm^{-1} (–)/1640 cm^{-1} (+), with smaller satellite bands at 1654 cm^{-1} (–) and 1630 cm^{-1} (+), appears almost not shifted in ^2H_2O. However, the relative intensity of the four signals appears altered, showing in ^2H_2O the same amplitude. The very weak difference band at 1700 cm^{-1} (–)/1684 cm^{-1} (+) is shifted in ^2H_2O to 1696 cm^{-1}

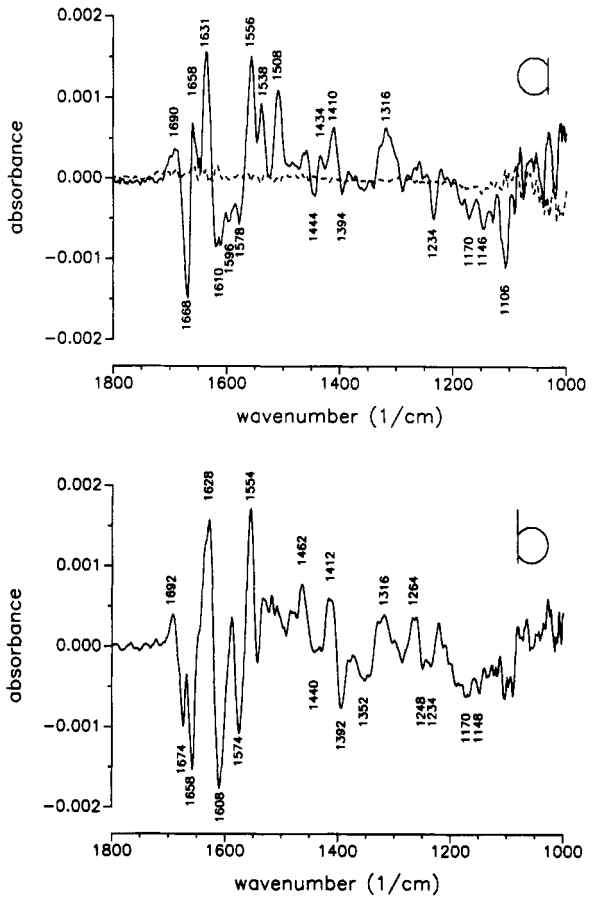

FIGURE 4: (a) (—) Reduced-minus-oxidized IR difference spectrum of a 50 mg/mL hemoglobin sample in phosphate buffer and 100 mM KCl, pH 7.0. The spectrum is the sum of several electrolysis cycles of 200 s at −300 mV and 600 s at +500 mV. (- - -) Reduced-minus-oxidized IR difference spectrum of the buffer solution in the presence of the MB-SME under the same conditions. (b) Reduced-minus-oxidized IR difference spectra in ^2H_2O (same conditions as in panel a).

(−)/1680 cm^{-1} (+). The spectral region between 1610 and 1540 cm^{-1} contains in ^1H_2O a very broad structure including several signals of very weak intensity at 1606 cm^{-1} (+), 1582 cm^{-1} (−), 1564 cm^{-1} (−) and 1548 cm^{-1} (+). This structure becomes much less broad and more simple in ^2H_2O, showing only three signals at 1596 cm^{-1} (−), 1570 cm^{-1} (−), and 1548 cm^{-1} (+), the latter of medium amplitude.

The positive band in ^1H_2O at 1530 cm^{-1} does not appear in the ^2H_2O spectrum, and the pair of signals in ^1H_2O at 1514 cm^{-1} (+) and 1500 cm^{-1} (+) is difficult to locate in the ^2H_2O spectrum. Other signals of moderate amplitude appear at much lower wavenumbers between 1100 and 1200 cm^{-1}. In this region the ^1H_2O spectrum shows a couple of structures at 1172 cm^{-1} (−)/1148 cm^{-1} (−) and 1106 cm^{-1} (+)/1100 cm^{-1} (−)/1088 cm^{-1} (+). These structures appear altered in ^2H_2O. The first one shows an additional signal at 1196 cm^{-1} (−) and the signal at 1100 cm^{-1} becomes much stronger. A weak difference signal at 1448 cm^{-1} (−)/1434 cm^{-1} (+) appears only in ^2H_2O.

Infrared Spectroscopy of Hemoglobin. Panels a and b of Figure 4 show the reduced-minus-oxidized IR difference spectra of a 50 mg/mL hemoglobin sample in ^1H_2O and ^2H_2O, respectively. These spectra were obtained with the MB-SME electrode as described for myoglobin. Figure 4a includes the reduced-minus-oxidized IR difference spectrum of the buffer solution in the presence of the MB-SME electrode, which shows the absence of any contribution in the IR difference spectra arising from the modifier. After the equilibration of the sample at +500 mV for 5 min, an IR single-beam spectrum of the oxidized state was recorded as a reference. A reductive potential of −300 mV was then applied for 300 s and a spectrum of the reduced state was recorded. In this case, however, it was necessary to apply +500 mV for at least 600 s in order to get the spectrum of the totally reoxidized sample. The spectra shown in Figure 4 apparently have very few features in common with those obtained with myoglobin (Figure 3). Hemoglobin spectra show a much more complicated pattern displaying several bands of high intensity. Furthermore, the changes in the spectrum upon deuteration are much higher than those observed for myoglobin.

The largest changes occur in the region between 1556 and 1690 cm^{-1}. The ^1H_2O spectrum in this region shows a very weak positive band at 1690 cm^{-1}, which is upshifted in ^2H_2O to 1692 cm^{-1}, and a strong difference band at 1668 cm^{-1} (−)/1631 cm^{-1} (+), with a satellite band at 1658 cm^{-1} (+). In this region, the spectrum recorded in ^2H_2O shows two high-intensity negative bands at 1674 and 1658 cm^{-1} and a positive band, also of high intensity, at 1628 cm^{-1} with a shoulder at 1636 cm^{-1}. The very broad negative band which appears in the ^1H_2O spectrum between 1620 and 1570 cm^{-1} contains at least three negative peaks at 1616, 1596, and 1578 cm^{-1}. This structure upon deuteration transforms into two well-defined negative bands at 1608 and 1574 cm^{-1}. The ^1H_2O spectrum shows three strong positive signals at 1556, 1538, and 1508 cm^{-1}. The ^2H_2O spectrum, however, only shows a positive signal at 1554 cm^{-1}.

The region between 1460 and 1350 cm^{-1} appears considerably altered in ^2H_2O. The ^1H_2O spectrum shows low intensity signals at 1444 cm^{-1} (−), 1434 cm^{-1} (+), 1410 cm^{-1} (+), and 1394 cm^{-1} (−). However, the ^2H_2O spectrum shows in this region signals of medium intensity at 1462 cm^{-1} (+), 1440 cm^{-1} (−), 1412 cm^{-1} (+), 1392 cm^{-1} (−), and 1352 cm^{-1} (−). The pair of signals at 1316 cm^{-1} (+) and 1234 cm^{-1} (−) appears unshifted in ^2H_2O; however, the ^2H_2O spectrum shows two additional signals at 1264 cm^{-1} (+) and 1248 cm^{-1} (−). The negative signals at 1170, 1146, and 1106 cm^{-1} are difficult to see in ^2H_2O.

As for myoglobin, spectra recorded at intermediate potentials showed the same signals with intermediate intensities. The amplitude of the infrared difference spectra corresponded in every case to 4% of the absorbance of the reduced-minus-oxidized Soret difference band at 434 nm.

When concentrations of protein higher than 50 mg/mL were used, the protein was irreversibly reduced. Under these conditions, it was also possible to get a reduced-minus-oxidized spectrum which showed a large increase of the difference signal at 1668 cm^{-1} (−)/1631 cm^{-1} (+) as well as of the satellite at 1658 cm^{-1} (+) which shifts to 1650 cm^{-1} (+) (data not shown).

DISCUSSION

(I) Electrochemical Behavior of the SMEs

The main objective of the electrochemical study described in this work has been the design of suitable surface-modified electrodes (SMEs) for reversible bulk electrolysis of highly concentrated samples of myoglobin and hemoglobin. A further goal was to obtain FTIR difference spectra in the absence of mediators in the protein solution, since difference bands from the mediators would mask the protein spectrum.

Heterogeneous electron transfer of hemoglobin has been described previously for MB, BCB, and JG platinum SMEs (Dong et al., 1989; Song & Dong, 1988; Zhu & Dong, 1990) and for myoglobin and hemoglobin at MB glassy carbon SMEs

and MV gold SMEs (Ye & Baldwin, 1988; Bowden et al., 1980). However, in none of these cases did the protein concentration in the samples exceed 12 mg/mL. We attribute the sometimes dramatically different behavior observed in our experiments mostly to the use of highly concentrated samples rather than to the different nature of the electrode surface.

MV-SMEs. MV-SMEs turned out to be the least stable electrodes, becoming quickly poisoned at myoglobin concentrations above 30 mg/mL. On the other hand, the heterogeneous electron transfer process is extremely slow as can be deduced from the large overpotentials required for both the reduction and oxidation process. The adsorption of small amounts of myoglobin at methyl viologen gold-foil electrodes has been demonstrated (Castner & Hawkridge, 1983).

BCB-SMEs. BCB-SMEs showed a high stability with highly concentrated samples of myoglobin, being able to carry out reversible bulk electrolysis with moderate reduction overpotentials in relatively short times. The value of the midpoint redox potential obtained for BCB in solution by cyclic voltammetry in the OTTLE cell was $E_{1/2}$ = –260 mV, 65 mV more negative than the standard redox potential of this compound at the same pH value as reported by Dong et al. (1989). A shift of the redox potential of the modifier toward more cathodic values has been observed in cyclic voltammograms of glassy carbon MB-SMEs in supporting electrolyte (Ye & Baldwin, 1988). Physical adsorption of BCB onto platinum electrodes has been reported (Dong et al., 1989) and the same may occur on gold. However, after successive cyclic scanning several layers of modifier were adsorbed onto the electrode surface until a backgroundlike voltammetric response was reached.

From the reductive potential stepping curves, the 50% reduction potential we obtained for myoglobin was $E_{50\%}$ = –270 mV. Since the standard redox potential of myoglobin at pH = 7.0 is –162 mV (Ye & Baldwin, 1988), it would be hard to believe that BCB could act as a redox mediator for the reduction of this protein. However, a mediated electron transfer mechanism through an excited triplet state which is created after BCB reduction has been proposed as being responsible for the interaction of hemoglobin with platinum BCB-SMEs (Dong et al., 1989).

In contrast to the high stability shown by platinum BCB-SMEs with low-concentration hemoglobin samples (Dong et al., 1989), the presence of large amounts of hemoglobin in the solution led to a fast poisoning of the gold BCB-SMEs, yielding the irreversible reduction of the protein.

MB-SMEs. The midpoint redox potential of MB in solution obtained by cyclic voltammetry in the OTTLE cell at pH = 7.0 was $E_{1/2}$ = –225 mV, more negative than the midpoint redox potential of MB in solution and very close to the values obtained for methylene blue adsorbed onto glassy carbon (Ye & Baldwin, 1988) and platinum (Song & Dong, 1988). Thus, this result indicates a very fast adsorption of the MB onto the gold grid surface just by dip-coating. As for BCB-SMEs, cyclic scanning with the electrode in MB solution leads to the adsorption of several layers of modifier, giving rise to a backgroundlike voltammetric response.

The reductive potential stepping of a myoglobin sample at the MB-SME showed a value for $E_{50\%}$ = –210 mV. Compared to the value obtained with the BCB-SMEs, the reduction overpotential has decreased by 60 mV. However, this overpotential is reduced to 28 mV after the reduction time of the reductive steps is increased. The oxidative potential stepping curve was slightly shifted toward more anodic values, showing a $E_{50\%}$ value of –180 mV, indicating a slightly slower oxidation rate.

MB-SMEs turned out to be relatively stable with highly concentrated samples of hemoglobin, since this protein undergoes a quasi-reversible heterogeneous electron transfer mechanism at the MB-SMEs.

From the reductive potential stepping curves, a value of $E_{50\%}$ of –140 mV was obtained, slightly more positive than the one obtained for diluted samples at the platinum MB-SMEs (Song & Dong, 1988). It has been described that in general the redox potentials of myoglobin and hemoglobin shift toward more negative values when the sample concentration is increased (Scheller et al., 1975); thus, this difference may be due to the fact that these authors have followed the titration of hemoglobin by the absorbance change at 550 nm, which is not the strongest peak. Moreover, in the range of concentrations between 50 and 100 mg/mL, we have not noticed significant shifts in the $E_{50\%}$ values obtained from the reductive potential stepping curves. However, the $E_{50\%}$ value we obtained has about 100 mV reduction overpotential with respect to the standard redox potential of hemoglobin at this pH.

The reductive potential stepping curve shows a Nernstian form but is much steeper than the one obtained for myoglobin, as could be expected for a theoretical number of electrons n = 4 transferred for hemoglobin. However, we obtained a value of n = 1.8, which is the same value obtained at the BCB-Pt electrodes by Dong et al., (1989).

The oxidative potential stepping curves showed a rather complicated pattern in which the full oxidation is considerably delayed. It is thus necessary to switch the anodic potential to +500 mV to obtain the completely oxidized sample in a moderately short time. It is interesting to note that the protein does not seem to be oxidized continuously with the anodic potential stepping. Instead, three different electrochemical processes can be distinguished. For the first oxidative process, the same $E_{50\%}$ value is obtained for all experiments as for the reductive potential stepping curve. This process involves an absorbance decrease of about 25% of the total oxidized-minus-reduced absorbance difference of the sample at 434 nm. The second oxidative process also involves 25% of the absorbance difference at 434 nm and was complete at +100 mV. The third redox process proceeded between +100 and +500 mV.

It appears possible that these electrochemical steps correspond to different redox states of the hemoglobin molecules depending upon the number of heme groups oxidized in the same molecule. On the other hand, this behavior could reflect the existence of a multilayer of weakly adsorbed protein onto the electrode surface, with the consequence that the closest ones are easier to reoxidize. The formation of a multilayer of adsorbed protein which acts in transferring electrons from the electrode to freely diffusible protein has been proposed for the electron transfer mechanism of myoglobin and hemoglobin at bare mercury electrodes (Scheller et al., 1975).

A partial and progressive degradation of the electrode has been observed after long and continuous working time. Degradation of the electrodes may lead to a delay in the global oxidation process, giving rise to a certain amount of irreversible reduced protein. We have observed in such cases that the first and second oxidation steps remained reproducible, whereas the third oxidation step was absolutely absent.

JG-SMEs. The behavior of highly concentrated samples of hemoglobin at the gold JG-SMEs was identical to that previously described for diluted samples at platinum JG-SMEs (Zhu & Dong, 1990).

(II) FTIR Difference Spectroscopy

Infrared Spectroscopy of Myoglobin. The small number of difference bands in the spectrum of myoglobin suggests a comparatively small conformational change upon the redox transition. Indeed, most of the signals can principally be attributed to transitions of amino acids surrounding the heme and to the heme ring itself.

The main difference band at 1664 cm^{-1} (–)/1640 cm^{-1} (+) is almost not shifted in ^2H_2O (2 cm^{-1} for the negative band at 1664 cm^{-1}). These bands are in a frequency range where the absorbance from peptide C=O stretching modes (amide I) is expected. They show two shoulders in ^1H_2O at 1654 cm^{-1} (–)/1630 cm^{-1} (+), which are also almost not shifted in ^2H_2O. Earlier FTIR studies (Susi & Byler, 1986) have shown that the amide I band for myoglobin in ^2H_2O appears at 1652 cm^{-1}, which is the value expected for the C=O stretching mode of α-helices. The secondary structure of myoglobin as deduced from crystallographic data is aproximately 80% α-helical structure and contains some turns which connect the different α-helix segments, whereas β-structures are completely absent (Levitt & Greer, 1977). However, more recently FTIR spectroscopic studies of the amide I band of this protein have revealed the existence of a small amount of disordered β-structures which were not expected from the crystallographic data (Goormaghtigh et al., 1990; Venyaminov & Kalnin, 1990a). The amide I band of myoglobin can be deconvoluted into components at 1657 and 1648 cm^{-1} which can be assigned to α-helical segments and at 1632 cm^{-1} for the β-sheet structures (Goormaghtigh et al., 1990). These values are rather similar to those reported for hemoglobin by Susi and Byler (1983), 1652 cm^{-1} for α-helical segments and 1638 and 1675 cm^{-1} for turns. The reason for the variation of the amplitude of the satellite signals in ^2H_2O is not very clear, but it could be due to the fact that deuteration of proteins can involves partial unfolding and refolding of the protein (Kalnin et al., 1990).

In agreement with the small conformational change proposed for myoglobin in its physiological reaction, no strong signals are detected in the amide II region (1600–1550 cm^{-1}). The very broad structure between 1606 and 1530 cm^{-1} becomes simpler and less broad with two well-defined negative weak bands in ^2H_2O at 1596 and 1570 cm^{-1}. This fact suggests the presence of a weak amide II band between 1530 and 1610 cm^{-1}, probably the positive signal at 1530 cm^{-1}, which may be completely shifted toward lower wavenumbers between 1430 and 1460 cm^{-1} in ^2H_2O. Indeed, the presence of a very weak difference signal at 1448 cm^{-1} (–)/1434 cm^{-1} (+) in the ^2H_2O spectrum agrees with this assumption. This broad structure may include also bands due to aromatic –HC=CH– stretching belonging to aromatic residues such as phenylalanine or tryptophan or heme vinyls (1606 cm^{-1}/^1H_2O) and –C=N– stretching of histidine (1596 cm^{-1}/^2H_2O), as well as the antisymmetric stretching of the –COO– of the heme-4 propionate (1564 cm^{-1}/^1H_2O). Unfortunately, the vibrational modes from the side chains of histidine and phenylalanine are only weak IR absorbers (Venyaminov & Kalnin, 1990b).

The presence of an extremely small difference band at 1700 cm^{-1} (+)/1684 cm^{-1} (–) may be due to the symmetric stretching of –COOH of the hydrogen-bonded heme-6 propionic acid. The bands arising from heme propionates are weak as compared to other heme proteins such as cytochrome *c* (Moss et al., 1990). This agrees with the weak interaction between these propionates and helix F deduced from NMR studies (La Mar et al., 1991). The pair of positive bands at 1514 and 1500 cm^{-1} could be due to ring vibration of tyrosine and phenylalanine [1515 and 1494 cm^{-1}, respectively (Venyaminov & Kalnin, 1990b)]. The sharp negative signal at 1100 cm^{-1}, once we exclude the possibility of oxygen presence in our cell [Fe–O–O stretching appears at 1107 cm^{-1} for hemoglobin and at 1103 cm^{-1} for myoglobin (Alben, 1978)], may belong to a mode of the heme ring since it appears in heme model compounds (Berthomieu, 1991). In these heme models, a pair of bands appears at 1149 and 1169 cm^{-1} which is very close to the 1148 and 1172 cm^{-1} bands observed in the myoglobin spectrum (Figure 3a). These bands have been assigned to a mode of the complex iron(III–porphyrin–methylimidazole and might well correspond to a mode of the complex Fe(III)–porphyrin–histidine.

The fact that all bands titrate in unison is in agreement with extremely fast conformational changes, with the accommodation of the protein molecules onto the electrode surface being the rate-limiting steps. A mechanism of a radial and a transversal diffusion of proteins toward punctual active sites of the electrodic surface where the electron transfer reaction can take place has been proposed by Bond et al. (1990).

Infrared Spectroscopy of Hemoglobin. In contrast to myoglobin, the FTIR difference spectra of hemoglobin show several signals of high intensity, presumably most of them belonging to amino acid residues. However, there are some features in the spectrum of hemoglobin which resemble some features of the myoglobin spectrum.

The main difference band in ^1H_2O at 1668 cm^{-1} (–)/1631 cm^{-1} (+) with a satellite band at 1650 cm^{-1} (+) appears in the region where the C=O stretching modes of the polypeptide backbone are expected. However, it is interesting to note that this structure is highly altered in ^2H_2O, in contrast to the normal behavior of an amide I band. The ^2H_2O spectrum in this region shows two strong negative bands at 1674 and 1658 cm^{-1} and a very strong positive band at 1628 cm^{-1}. As for myoglobin, the secondary structure of hemoglobin as derived from crystallographic data consists of 80% α-helices, some turns connecting the α-helical segments, and no β-structures (Levitt & Greer, 1977). Although no quantitative determination of the secondary structure of hemoglobin by FTIR spectroscopy has been published, we could expect the existence of some β-structures as for myoglobin. Susi and Byler (1983) have found that the amide I of bovine hemoglobin can be deconvoluted into three components at 1652 cm^{-1} for α-helical segments and 1675 and 1638 cm^{-1} for turns. A band at 1623 cm^{-1} was found in β-lactoglobulin by the same authors, who suggested that this signal may be associated with a special kind of β-structure.

The weak positive signal at 1690 cm^{-1} could be assigned to symmetric stretching of –COOH of heme-6 propionic acid. The broad structure in ^1H_2O between 1610 and 1578 cm^{-1} may include, as in the case of myoglobin, –CH=CH– stretching of aromatic rings or heme vinyls, –C=N– stretching of histidine, and antisymetric stretching of –COO– heme-4 propionate. The positive and strong signal at 1556 cm^{-1} in ^1H_2O, which is shifted in ^2H_2O to 1554 cm^{-1}, has no correspondence in the myoglobin spectrum and could arise from vibrations of the indole ring of tryptophan-β37, which is the $\alpha_1\beta_2$ interface and gives rise to a Raman signal at 1555 cm^{-1} (Spiro et al., 1990). The signal at 1538 cm^{-1} appears only in the ^1H_2O spectrum and could arise from –C—N–/–N—H– stretching modes of peptides (amide II). This signal appears in the ^2H_2O spectrum as a difference signal at 1462 cm^{-1} (+)/1440 cm^{-1} (–). The strong positive signal in ^1H_2O at 1508 cm^{-1} could be due to ring vibrations of tyrosine-α42 (1515 cm^{-1}) and phenylalanine (1494 cm^{-1}). Phenylalanine residues can be found in the proximity of the $\alpha_1\beta_2$ interface

(Phe α46 and Phe β45) and the Phe 1CD in the heme cavity. In fact, the aromatic residues at the $\alpha_1\beta_2$ interface play a very important role in the transition R → T. This transition proceeds through an intermediate state which involves changes in the hydrogen bonding of the aromatic residues of the interface (Chang et al., 1989). As in the myoglobin spectrum, the ^1H_2O spectrum of hemoglobin shows the heme bands at 1146, 1170, and 1106 cm^{-1}.

When comparing the hemoglobin spectra with those obtained with myoglobin, in hemoglobin the amplitude of the IR difference spectrum is about 4% of the difference absorbance in the Soret band. That agrees with the existence of a similar conformational change in each of the four heme moieties besides the quaternary conformational change which involves the subunit interfaces. The movement of helix F away from the heme in the transition R → T is 1 Å in hemoglobin, whereas for myoglobin it is 0.1 Å (Spiro et al., 1990). That could be the reason for the appearance of several signals of high amplitude in the hemoglobin spectrum, in contrast to the myoglobin spectrum.

CONCLUSIONS

The redox-induced IR difference spectra of the well-known heme proteins myoglobin and hemoglobin have demonstrated that the combination of protein electrochemistry and IR spectroscopy provides a considerable potential for the study of functionally related protein conformation changes. With electrochemical techniques at surface-modified electrodes avoiding redox mediators (which would interfere with their IR absorbance), quantitative and reversible redox reactions were achieved. The IR difference bands observed here are directly related to the redox process(es) as evidenced by their lependence on the applied potential.

Resonance Raman spectra of heme proteins have revealed heme bands as markers for the redox state. In addition, UV resonance Raman spectra have provided evidence for different protein conformations. We would like to emphasize, however, that in the IR difference spectra presented here bands from the heme, from peripheral heme groups such as the propionates, from amino acid side chain groups, and from the polypeptide backbone are contributing. The multitude of IR modes characteristic for the redox state of the hemes can ideally serve as probes not only for the local heme environment and interaction but also for the interaction of different subunits of the protein, as in the case of hemoglobin.

Clearly, the analysis of the FTIR difference spectra is far from being complete. We regard, however, FTIR difference spectroscopy of these (and even more complex) redox proteins as being complementary to high-resolution structure analysis. Since neither crystalline nor highly purified samples are required for IR difference spectroscopy, the molecular mechanisms accompanying the redox transition can be studied at conditions close to the native reactions, with the native redox partners, and even for solubilized or membrane-bound proteins. The information from redox-induced FTIR difference spectra thus complements and supplements the structural information obtained for example from the crystalline state and may lead to a consistent picture of a given structure leading to a specific function.

ACKNOWLEDGMENT

We thank Professor Victor M. Fernández, Instituto de Catálisis y Petroleoquimica, Madrid, Spain, and Professor W. Kreutz, Institut für Biophysik, for encouraging support.

REFERENCES

Alben, J. O. (1978) in *The porphyrins* (Dolphin, D., Ed.) Vol. III, pp 323–347, Academic Press, New York.
Antonini, E., Wyman, J., Brunori, M., Taylor, J. F., Rossi-Fanelli, A., & Caputo, A. (1964) *J. Biol. Chem. 239*, 907–912.
Antonini, E., Bucci, E., Fronticelli, C., Wyman, J., & Rossi-Fanelli, A. (1965) *J. Mol. Biol. 12*, 375–384.
Banerjee, R., & Cassoly, R. (1969a) *J. Mol. Biol. 42*, 337–349.
Banerjee, R., & Cassoly, R. (1969b) *J. Mol. Biol. 42*, 351–361.
Barker, P. D., di Gleria, K., Hill, H. A. O., & Lowe, V. J. (1990) *Eur. J. Biochem. 190*, 171–175.
Baymann, F., Moss, D., & Mäntele, W. (1991) *Anal. Biochem. 199*, 269–274.
Berthomieu, C. (1991) Doctoral Thesis, Pierre and Marie Curie University, Paris.
Bond, A. M., Hill, H. A. O., Page, D. J., Psalti, I. S. M., & Walton, N. J. (1990) *Eur. J. Biochem. 191*, 737–742.
Bowden, E. F., Hawkridge, F. M., & Blount, H. N. (1980) *Bioelectrochem. Bioenerg. 7*, 447–457.
Brunori, M., Antonini, E., Wyman, J., Zito, R., Taylor, J. F., & Rossi-Fanelli, A. (1964) *J. Biol. Chem. 239*, 2340–2344.
Brunori, M., Taylor, J. F., Antonini, E., Wyman, J., & Rossi-Fanelli, A. (1967) *J. Biol. Chem. 242*, 2295–2300.
Castner, J. E., & Hawkridge, F. M. (1983) *J. Electroanal. Chem. 143*, 217–232.
Chang, S., Park, Y. D., Liu, G., & Spiro, T. G. (1989) *J. Am. Chem. Soc. 111*, 3457–3459.
Cotton, T. M., Schultz, S. G., & van Duyne, R. P. (1980) *J. Am. Chem. Soc. 102*, 7960–7962.
Dayhoff, M. O. (1972) *Atlas of Protein Sequence and Structure*, Vol. 5, National Biochemical Foundation, Washington, DC.
di Gleria, K., Hill, H. A. O., Lowe, V. J., & Page, D. J. (1986) *J. Electroanal. Chem. 213*, 333–338.
Dong, S., Zhu, Y., & Song, S. (1989) *Bioelectrochem. Bioenerg. 21*, 233–243.
Goormaghtigh, E., Cabiaux, V., & Ruysschaert, J. M. (1990) *Eur. J. Biochem. 193*, 409–420.
Hill, H. A. O., & Lawrance, G. A. (1989) *J. Electroanal. Chem. 270*, 309–318.
Kalnin, N. K., Baikalov, L. A., & Venyaminov, S. Y. (1990) *Biopolymers 30*, 1273–1280.
La Mar, G. N., Hanksson, J. B., Dugad, L. B., Lidell, P. A., Venkataramana, N., & Smith, K. N. (1991) *J. Am. Chem. Soc. 113*, 1544–1550.
Landrum, H. L., Salmon, R. T., & Hawkridge, F. M. (1977) *J. Am. Chem. Soc. 99*, 3154–3158.
Levitt, M., & Greer, J. (1977) *J. Mol. Biol. 114*, 181–293.
Moss, D., Nabedryk, E., Breton, J., & Mäntele, W. (1990) *Eur. J. Biochem. 187*, 565–572.
Phillips, S. E. V. (1980) *J. Mol. Biol. 142*, 531–554.
Shaanan, B. (1983) *J. Mol. Biol. 171*, 31–59.
Scheller, F., Jänchen, M., Lampe, J., Prümke, H. J., Blanck, J., & Palecek, E. (1975) *Biochim. Biophys. Acta 412*, 157–167.
Song, S., & Dong, S. (1988) *Bioelectrochem. Bioenerg. 19*, 337–346.
Spiro, T. G., Smulevich, G., & Chang, S. (1990) *Biochemistry 29*, 4497–4508.
Stargardt, J. F., Hawkridge, F. M., & Landrum, H. L. (1978) *Anal. Chem. 50*, 930–932.
Stein, P., Terner, J., & Spiro, T. G. (1982) *J. Phys. Chem. 86*, 168–170.
Stellwagen, E. (1978) *Nature 275*, 73–74.
Susi, H., & Byler, D. M. (1983) *Biochem. Biophys. Res. Commun. 115*, 391–397.
Susi, H., & Byler, D. M. (1986) in *Methods in Enzymology* (Hirs, C. H. W., & Timasheff, S. N., Eds.) Vol. 130, pp 290–311, Academic Press Inc., New York.
Takano, T. (1977a) *J. Mol. Biol. 110*, 537–568.
Takano, T. (1977b) *J. Mol. Biol. 110*, 569–584.
Venyaminov, S. Y., & Kalnin, M. N. (1990a) *Biopolymers 30*, 1243–1257.
Venyaminov, S. Y., & Kalnin, M. N. (1990b) *Biopolymers 30*, 1259–1271.
Ye, J., & Baldwin, R. P. (1988) *Anal. Chem. 60*, 2263–2268.
Zhu, Y., & Dong, S. (1990) *Bioelectrochem. Bioenerg. 24*, 23–31.